Published in final edited form as:
J Am Chem Soc. 2008 September 24; 130(38): 12775–12782. doi:10.1021/ja8037849.

Cyclic Ruthenium-Alkylidene Catalysts for Ring-Expansion Metathesis Polymerization

Andrew J. Boydston, **Yan Xia**, **Julia A. Kornfield**, **Irina A. Gorodetskaya**, and **Robert H. Grubbs***
Arnold and Mabel Beckman Laboratory of Chemical Synthesis, Division of Chemistry and Chemical Engineering, California Institute of Technology, Pasadena, California 91125

Abstract

A series of cyclic Ru-alkylidene catalysts have been prepared and evaluated for their efficiency in ring-expansion metathesis polymerization (REMP). The catalyst structures feature chelating tethers extending from one N-atom of an imidazolylidine ligand to the Ru metal center. The catalyst design is modular in nature, which provided access to Ru-complexes having varying tether lengths, as well as electronically different NHC ligands. Structural impacts of the tether length were unveiled through ^{1}H NMR spectroscopy as well as single-crystal X-ray analyses. Catalyst activities were evaluated via polymerization of cyclooctene and key data are provided regarding propagation rates, intramolecular chain-transfer, and catalyst stabilities, three areas necessary for the efficient synthesis of cyclic poly(olefin)s via REMP. From these studies, it was determined that while increasing the tether length of the catalyst leads to enhanced rates of polymerization, shorter tethers were found to facilitate intramolecular chain-transfer and release of catalyst from the polymer. Electronic modification of the NHC via backbone saturation was found to enhance polymerization rates to a greater extent than did homologation of the tether. Overall, cyclic Ru-complexes bearing 5- or 6-carbon tethers and saturated NHC ligands were found to be readily synthesized, bench-stable, and highly active catalysts for REMP.

Keywords

cyclic polymers; metathesis; ring-opening polymerization; ruthenium

Introduction

The exploration of Ru-based metathesis catalysts has opened doorways to multiple areas of synthetic and polymer chemistry.[1,2] Advances in these areas have been made possible via development of new catalyst scaffolds based upon bis(phosphine) complex **1** (Figure 1), or those bearing N-heterocyclic carbene (NHC) ligands such as **2** and **3**. The introduction of catalysts based on **1** – **3**, but predisposed for specific tasks, has further expanded the potential of olefin metathesis. For example, areas such as solid-supported catalysis,[3] asymmetric olefin metathesis,[4] tandem catalysis,[5] living polymerization,[1a,6] acyclic diene metathesis,[7] and stereoselective cross-metathesis (CM) have each benefited from breakthroughs in catalyst design, development, and application.[8]

Recently, a Ru-based catalyst design was reported that featured a chelating N-to-Ru tether (Figure 2).[9] Whereas the catalytic activities of $\mathbf{4}_{\mathbf{cyc}}$ – $\mathbf{6}_{\mathbf{cyc}}$ have not been explored, $\mathbf{7}_{\mathbf{cyc}}$ was

rhg@caltech.edu.

found to mediate the synthesis of cyclic polymers from cyclic monomers (Scheme 1).[10,11] This ring-*expansion* metathesis polymerization (REMP) afforded the ability to produce cyclic polymers on large scale from diverse, readily-available cyclic monomers.[12,13] While the high catalytic activity of $\mathbf{7_{cyc}}$ was desirable, the synthesis and storage of this compound were complicated by instability.

To realize the potential in the area of cyclic polymer chemistry, catalysts should be readily synthesized in good yields, be easily purified to eliminate any acyclic contaminants, and have an appropriate balance of stability (e.g., during storage as well as polymerizations) and activity. To address issues of stability, we envisioned that catalysts with shorter tether lengths, such as $\mathbf{4_{cyc}}$, $\mathbf{5_{cyc}}$, and $\mathbf{6_{cyc}}$, which contain 4-, 5-, and 6-carbon tethers, respectively, may be advantageous. A potential drawback, however, is that this may be accompanied by decreased catalytic activities. Therefore, we designed catalysts to incorporate two key structural features, shortened tether lengths and saturated NHC backbones, expected to synergistically provide REMP catalysts of high stabilities and activities.[14]

We also hoped to further elucidate the mechanism by which REMP proceeds through judicious catalysts design. Initially, REMP was proposed to proceed via a ring-expansion initiation event from a cyclic Ru-alkylidene catalyst (Scheme 1) and propagate as cyclic monomers were incorporated into a growing cyclic polymer. Upon consumption of monomer, a final catalyst release step would provide the original catalyst and the desired cyclic polymer. The polymerization mechanism depicted in Scheme 1 has several intriguing features including: 1) opening of a chelated Ru-alkylidene catalyst, 2) propagation with the prospect of competing intramolecular chain-transfer events, and 3) a final release of the original catalyst via intramolecular CM.

Many scenarios are consistent with Scheme 1, depending on the relative rates of initiation, propagation, intramolecular chain-transfer, and catalyst release. Initial studies using catalyst $\mathbf{7_{cyc}}$ demonstrated the ability to control polymer molecular-weight (MW) using the monomer/catalyst loading.[11] This corresponds to a regime in which nearly complete initiation occurs, and catalyst release does not take place prior to complete monomer consumption. Another key observation was that after complete conversion of monomer, the MW of the cyclic polymers progressively decreased in the presence of $\mathbf{7_{cyc}}$, indicating significant amounts of intramolecular chain-transfer (Scheme 1). Alternatively, if the rate of propagation is much greater than that of initiation, and the rates of intramolecular chain-transfer and catalyst release are negligible, then all monomer species may be incorporated into a number of macrocycles equal to the number of catalyst molecules that initiated. This latter scenario would yield cyclic polymers in which Ru is incorporated into the backbone. Finally, a catalyst that shows relatively rapid release from a propagating cyclic chain may be expected to initiate, propagate (e.g., oligomerize), and then release, ultimately providing multiple polymer rings from each catalyst complex. Therefore, understanding how the catalyst design influences the relative kinetics of these processes is central to controlling the nature and distribution of products obtained via REMP.

To better understand each of the mechanistic aspects of REMP, and provide guidance for REMP catalyst design, we sought to investigate a homologous series of cyclic catalysts of varying N-to-Ru tether lengths (Figure 2). The tether length may be central in controlling structural features of the catalyst such as: 1) inherent ring-strain in the cyclic Ru-complexes, 2) relative orientations of the NHC and PCy_3 ligands about the metal center, and 3) rotation about the Ru-alkylidene (i.e., Ru=C-R) bond. As will be discussed below, a combination of NMR spectroscopy and single-crystal X-ray analyses of cyclic catalysts ultimately revealed key connections between their structures and activities.

Considering each step in the REMP cycle, it was expected that the tether length ideal for polymerization activity might be unfavorable for catalyst release. Specifically, intramolecular metathesis to reform and release the initial catalyst from the polymer is expected to be most efficient for shorter tether lengths. In contrast, increased tether lengths may be beneficial for polymerization rates, considering longer tethers may increase ring-strain of the catalyst or provide necessary flexibility within the structure. Encouraged by the modular nature of the NHC ligand, and the possibility of controlling REMP catalyst activities via tether length, we prepared and analyzed a homologous series of cyclic REMP catalysts (**4**$_{cyc}$ – **7**$_{cyc}$, Figure 2), as well as analogues possessing saturated imidazolinylidene ligands. Herein, we report the study of their activities in various steps of the REMP cycle, as well as key structure-activity relationships.

Results and Discussion

Catalyst Syntheses

The syntheses of complexes **4**$_{cyc}$ and **5**$_{cyc}$ were previously described by Fürstner.[9] To our knowledge, however, their catalytic activity has not been reported. Catalysts **6**$_{cyc}$ and **7**$_{cyc}$ were prepared analogously, as described in Scheme 2. The corresponding imidazolium salts (**8**) were first obtained by alkylation of 1-mesitylimidazole.[15] Ligand exchange was then achieved via deprotonation of the imidazolium salt, followed by addition of bis(phosphine) complex **1** (**8**/**1** molar ratio = 2:1) to give "open" complexes **4**$_{acyc}$ – **7**$_{acyc}$.[10, 16] In general, ligand exchange proceeded smoothly and the desired non-chelated complexes were isolated in good yields after chromatography on silica gel.[17,18] Intramolecular metathesis/cyclization was conducted in a PhH/pentane mixture (1:15 v/v) at 70 °C and 0.001 M to give the final "closed" complexes **4**$_{cyc}$ – **7** $_{cyc}$. Each of the catalysts could be purified by chromatography on silica gel, however, purification of **4**$_{cyc}$ – **6**$_{cyc}$ was more efficiently accomplished via recrystallization from Et_2O/pentane.[15]

We noted that the efficiency of cyclization of open complexes **4**$_{acyc}$ – **7**$_{acyc}$ to give cyclic catalysts **4**$_{cyc}$ – **7**$_{cyc}$ is highly dependent on the tether length (Table 1). Ostensibly, the ability of an open complex to undergo intra- versus intermolecular metathesis events gives some indication of the tendency for the proposed catalyst release step in Scheme 1. Table 1 summarizes the results of cyclization reactions for each catalyst at 0.01 and 0.001 M. In each case, yields were markedly improved at lower concentration (0.001 M) as determined by ^{1}H NMR analysis of the crude reaction mixtures. At 0.01 M, additional alkylidene peaks were observed via ^{1}H NMR spectroscopy that were upfield of signals characteristic of **1**, **4**$_{acyc}$ – **7**$_{acyc}$, or **4**$_{cyc}$ – **7** $_{cyc}$. These signals may be attributed to CM products such as those arising from CM involving styrene (formed as a product in the cyclization step), or the terminal olefin on an NHC ligand with another Ru-complex. As expected, these intermolecular metathesis events were significantly diminished at lower concentration. Prolonged reaction times did not result in increased yields of the desired cyclic species, rather decomposition was observed. It is worth noting that in the case of **7**$_{acyc}$, no product was observed when cyclization was conducted at 0.01 M. Therefore, catalyst release during REMP may be slow in comparison with other chain-transfer events when **7**$_{cyc}$ is employed.[19]

Considering the enhanced activity observed from saturation of the NHC backbone (cf. **2** and **3**),[14] we were motivated to investigate cyclic catalysts incorporating this design feature. As depicted in Scheme 3, a $PhCH_3$ solution of *N*-mesitylethylenediamine (**9**)[20] was treated with $HC(OEt)_3$ in the presence of catalytic PTSA and stoichiometric bromo-olefin at 110 °C. This one-pot procedure effected cyclization and alkylation to provide the imidazolinium salts **10** in excellent yields.[21] Unfortunately, attempts at direct deprotonation of **10** using KHMDS in the presence of bis(phosphine) complex **1** were complicated by NHC dimerization and provided low yields of the desired products.[22] Alternatively, treatment of **10** with NaH in $CHCl_3$ cleanly

provided neutral adducts **11**.[23] Heating THF solutions of **11** (0.001 M) in the presence of **1** (**11**/**1** molar ratio = 2:1) accomplished ligand exchange as well as cyclization to provide the desired cyclic catalysts $\mathbf{5_{cyc}}\cdot\mathbf{H_2}$ and $\mathbf{6_{cyc}}\cdot\mathbf{H_2}$ in 46 and 57% overall yields, respectively.[24] Although $\mathbf{5_{cyc}}\cdot\mathbf{H_2}$ and $\mathbf{6_{cyc}}\cdot\mathbf{H_2}$ were each isolable via chromatography on silica gel, both were found to be crystalline solids and were routinely recrystallized by slow addition of pentane into saturated PhH solutions of the complexes. Similar to $\mathbf{5_{cyc}}$ and $\mathbf{6_{cyc}}$, the saturated catalysts $\mathbf{5_{cyc}}\cdot\mathbf{H_2}$ and $\mathbf{6_{cyc}}\cdot\mathbf{H_2}$ displayed good stability both in the solid-state and in solution.[25]

Structural Analyses

The structural impacts of changing the tether lengths of catalysts $\mathbf{4_{cyc}}$ – $\mathbf{7_{cyc}}$ resulted in significant differences in catalyst activities (see polymerization studies below for more discussion). In addition to understanding the structure-activity relationships pertaining to REMP catalysts, a more general understanding of catalyst architecture may lead to breakthroughs in catalyst design as well as fundamental mechanistic insights of olefin metathesis. Cyclic catalysts $\mathbf{4_{cyc}}$ – $\mathbf{6_{cyc}}$ were found to show tether length-dependent trends in three key structural parameters summarized in Table 2:1) rotation about the Ru1-C2 bond, 2) the C1-Ru1-P1 bond angle, and 3) the Ru-C1 bond length (Figure 3).[26]

Although many structural features of $\mathbf{4_{cyc}}$ – $\mathbf{7_{cyc}}$ are best observed via solid-state analysis, rotation about the Ru1-C2 bond is manifested in the coupling constants between the P1 and H2 (i.e., the alkylidene proton, bonded to C2) atoms in the ^{1}H NMR spectra (Table 2 and Figure 3). Complexes $\mathbf{4_{cyc}}$ and $\mathbf{5_{cyc}}$, which were previously characterized in solution and solid-state,[9] displayed coupling constants of $^3J_{H2,P1}$ = 14.1 and 10.5 Hz (solvent = C_6D_6), respectively. The smaller coupling constant observed from complex $\mathbf{5_{cyc}}$, in comparison with $\mathbf{4_{cyc}}$, indicated that the corresponding atoms in the former are closer to a perpendicular arrangement. Consistent with this trend, a smaller coupling constant was observed in the ^{1}H NMR spectrum of $\mathbf{6_{cyc}}$ (i.e., $^3J_{H2,P1}$ = 5.1 Hz), indicating that the alkylidene proton (H2) was projected nearly perpendicular to the Ru1-P1 bond. The ^{1}H NMR spectrum of $\mathbf{7_{cyc}}$ revealed a coupling constant of $^3J_{H2,P1}$ = 10.2 Hz, which may be ascribed to the increased ring size (cf. $\mathbf{6_{cyc}}$) inducing twist about the Ru1-C2 bond.[27]

To further investigate the structures of the cyclic catalysts, we compared single-crystal X-ray data of $\mathbf{4_{cyc}}$ – $\mathbf{6_{cyc}}$, as well as saturated analogues $\mathbf{5_{cyc}}\cdot\mathbf{H_2}$ and $\mathbf{6_{cyc}}\cdot\mathbf{H_2}$.[26] The crystal structures of these complexes confirmed a variable degree of rotation about the Ru1-C2 bond, as determined from the Cl2-Ru-C2-C3 dihedral angles (Table 2). Overall, for $\mathbf{4_{cyc}}$ – $\mathbf{6_{cyc}}$, decreased $^3J_{H2,P1}$ values corresponded to decreased dihedral angles suggesting that the solution and solid-state structures of the catalysts are similar. It should be noted that while the $^3J_{H2,P1}$ values observed from $\mathbf{5_{cyc}}\cdot\mathbf{H_2}$ and $\mathbf{6_{cyc}}\cdot\mathbf{H_2}$ were consistent with each complex's respective unsaturated analogue, solid-sate analysis revealed that the Cl2-Ru-C2-C3 dihedral angles were not consistent with the trend observed from the unsaturated series.

Stepwise increase in the tether lengths was found to cause increasing nonlinearity in the C1-Ru1-P1 bond angles. Specifically, catalysts $\mathbf{4_{cyc}}$, $\mathbf{5_{cyc}}$, and $\mathbf{6_{cyc}}$ have C1-Ru1-P1 bond angles of 171.0, 166.0, and 163.3°, respectively. One rationale for this trend may be that increasing the tether length caused the NHC ligand to tilt to accommodate the increased steric demand of the tether. A consequence of this tilt is that the Mes group is forced closer to the PCy_3 group which may facilitate dissociation of the phosphine during initiation (see below for a comparison of catalyst activities).[14a] In addition, the tilted conformation may be difficult to restore which would hinder catalyst release and thus manifest in more rapid polymerization. Steric demands also resulted in discernable increases in the Ru1-P1 and Ru1-C1 bond lengths as the tether length was increased. For example, upon extension of the tether, the Ru1-C1 bond length increased from 2.076 Å for $\mathbf{4_{cyc}}$ to 2.113 Å for $\mathbf{6_{cyc}}$. The saturated catalysts, $\mathbf{5_{cyc}}\cdot\mathbf{H_2}$ and

6_{cyc}·H_2, showed changes in their Ru1-P1 and Ru1-C1 bond lengths that were consistent with those observed in the unsaturated series.

Ring-Expansion Metathesis Polymerization

To our knowledge, the catalytic activities of complexes **4_{cyc}** – **6_{cyc}** have not been explored in either small-molecule or polymer syntheses. In addition, electronic variants such as saturation of the NHC backbone have not been investigated. To compare the activities of **4_{cyc}** – **7_{cyc}** in REMP, we examined their relative efficiencies in the polymerization of cyclooctene (COE) to poly(cyclooctene) (PCOE). As can be seen from the data presented in Figure 4, the relative efficiencies of the catalysts showed a strong dependence on the length of the chelating tether.[28] In general, increased tether length was accompanied by an increase in catalytic activity. For example, comparison of the unsaturated catalysts revealed the time required to reach >95% conversion was nearly 24 h for **4_{cyc}** (green line), approximately 8 h for **5_{cyc}** (purple line) and **6_{cyc}** (blue line), and less than1 h for **7_{cyc}** (red line).

Saturation of the NHC backbone was found to dramatically increase catalyst activity. As expected, **5_{cyc}·H_2** and **6_{cyc}·H_2** each displayed faster polymerization rates than their unsaturated analogues **5_{cyc}** and **6_{cyc}**, respectively (Figure 4). Surprisingly, the rate acceleration resulting from NHC saturation appeared to be greater than for homologation of the tether length. Specifically, **6_{cyc}·H_2** was found to achieve >95% conversion in shorter reaction times than did **7_{cyc}**. Similarly, **5_{cyc}·H_2** was found to be a more active polymerization catalyst than **6_{cyc}**. Overall, the data revealed that judicious combinations of shorter tether lengths (i.e., 5- or 6-carbon tethers) and NHC backbone saturation (e.g., **5_{cyc}·H_2** and **6_{cyc}·H_2**) provided a desirable balance of catalyst stabilities, synthetic accessibility, and activities.

Catalyst stability takes on particular importance in REMP as decomposition of the catalyst before, during, or after polymerization could potentially lead to linear polymers, instead of the envisioned macrocycles. In addition, relative stabilities are important factors in the general development of new metathesis catalysts, especially considering that catalyst stability and activity are often inversely related.[29] To explore the stabilities of REMP catalysts **4_{cyc}** – **7_{cyc}** during polymerization reactions, we plotted the ln([COE]) versus time for REMP of COE (Figure 5). The logarithmic plots were found to be linear (R^2 values ranged from 0.969 – 0.997) between 20 and 80% conversion of COE to PCOE, indicating that catalyst decomposition was negligible in all cases during the time of the polymerization reactions. Closer examination of the plots revealed that the only discernable deviations from linearity (i.e., pseudo-first-order rate kinetics) involved apparent increases in the rate of monomer consumption. This observation can be rationalized by a relatively slow initiation period which would manifest in a gradual increase in the number of propagating polymer chains, and concomitant increase in the rate of conversion.

Catalyst Release

A unique aspect of REMP, in comparison with ring-*opening* metathesis polymerization (ROMP), is the requirement for an intramolecular chain-transfer event with the olefin nearest to the NHC to release the initial cyclic catalyst and provide a cyclic polymer free of Ru (Scheme 1). While removal of Ru from linear polymers obtained via ROMP can be done efficiently using a terminating agent, such as ethyl vinyl ether, this method is incompatible with REMP as it may result in linear polymer formation.[30] Given the importance of catalyst release from the cyclic polymers, we investigated each catalyst's propensity to undergo intramolecular cyclization during polymerization that would be indicative of the catalyst's ability to be released from a polymer.

We envisioned that conducting polymerizations using "open" catalysts $\mathbf{5_{acyc}}$ – $\mathbf{7_{acyc}}$ would provide insight into each catalyst's ability to perform intramolecular CM to release "closed" catalysts $\mathbf{5_{acyc}}$ – $\mathbf{7_{acyc}}$.[31] Propagation via growing Ru-alkylidene species **A** (Scheme 4) would inherently compete with catalyst cyclization (e.g., $\mathbf{A} \rightarrow \mathbf{5_{cyc}} + \mathbf{B}$), and provide an indication of each catalyst's propensity to be released from the polymer chain.

To investigate, we conducted polymerizations of COE using open catalysts $\mathbf{5_{acyc}}$ – $\mathbf{7_{acyc}}$ in CD_2Cl_2 at 40 °C ($[M/C]_0$ = 250:1, $[M]_0$ = 0.5 M) and monitored the alkylidene region of the ^{1}H NMR spectrum as the reactions progressed. Each Ru-complex shown in Scheme 4 was identified by characteristic chemical shifts of the corresponding alkylidene protons. In CD_2Cl_2, complexes $\mathbf{5_{acyc}}$ – $\mathbf{7}_{\mathbf{acyc}}$ gave sharp benzylidene resonances as singlets at δ = 19.30 ppm, whereas propagating species (**A**) displayed broad multiplets at δ = 18.69 ppm. Cyclic catalysts $\mathbf{5_{cyc}}$, $\mathbf{6_{cyc}}$, and $\mathbf{7_{cyc}}$ displayed signals at δ = 20.23, 19.35, and 19.67 ppm, respectively, with multiplicities matching those in Table 2.

We first examined open catalysts $\mathbf{6_{acyc}}$ and $\mathbf{7_{acyc}}$ as these were representative of the most active cyclic catalysts ($\mathbf{6_{cyc}}$ and $\mathbf{7_{cyc}}$, respectively) for this series. Catalysts $\mathbf{6_{acyc}}$ and $\mathbf{7_{acyc}}$ gave similar results, and polymerization of COE was found to reach completion faster than did cyclization of $\mathbf{6_{acyc}}$ and $\mathbf{7_{acyc}}$ to give $\mathbf{6_{cyc}}$ and $\mathbf{7_{cyc}}$, respectively. Specifically, complete conversion of COE was achieved in less than 5 min for each catalyst.[32] The mole fraction of cyclic catalyst ($\mathbf{6_{cyc}}$/$\mathbf{7_{cyc}}$) observed at this point, however, was only ca 10%, relative to $\mathbf{6_{acyc}}$/$\mathbf{7_{acyc}}$ (ca 30%) and **A** (ca 60%). Continued heating resulted in diminished amounts of $\mathbf{6_{acyc}}$/$\mathbf{7_{acyc}}$ and $\mathbf{6_{cyc}}$/$\mathbf{7_{cyc}}$ in each case, with concomitant increases in the relative amounts of **A**. As will be discussed in the next section, the continued progression to form **A** may have been due to incorporation of free cyclic catalyst into the polymer chains. After ca 1 h, only trace amounts of cyclic species $\mathbf{6_{cyc}}$/$\mathbf{7_{cyc}}$ could be observed. Overall, these results suggested that cyclization is not favored over polymerization for catalysts bearing 6- or 7-membered tethers, and that cyclization to release catalyst $\mathbf{6_{cyc}}$ or $\mathbf{7_{cyc}}$ after polymerization is not likely.

We next investigated the behavior of $\mathbf{5_{acyc}}$ under the same conditions as described above. In contrast to the longer tethered analogues $\mathbf{6_{acyc}}$ and $\mathbf{7_{acyc}}$, polymerization reactions using $\mathbf{5_{acyc}}$ revealed much faster cyclization (to give $\mathbf{5_{cyc}}$) relative to polymerization. Figure 6 shows the mole fraction of each catalytic species ($\mathbf{5_{acyc}}$, **A**, and $\mathbf{5_{cyc}}$) as well as the conversion of COE to PCOE over time. As can be seen, almost complete formation of cyclic catalyst $\mathbf{5_{cyc}}$ was observed after ca 45 min, at which time the polymerization had reached only 48% conversion. Moreover, the amount of catalytic species within the polymer chains (**A**) quickly diminished to nearly undetectable amounts. The data presented in Figure 6 supports that cyclization to form $\mathbf{5_{cyc}}$ is favored over propagation and that the background rate of cyclization (i.e., $\mathbf{5_{acyc}} \rightarrow \mathbf{5_{cyc}}$) is also significant for this catalyst. In addition, the persistent amount of $\mathbf{5_{cyc}}$ that is observed relative to propagating species (**A**) suggested that incorporation of $\mathbf{5_{cyc}}$ into existing polymer chains is unlikely. The continued conversion of COE to PCOE, with persistent observation of only $\mathbf{5_{cyc}}$, suggested that this cyclic catalyst reached an equilibrium between propagating (e.g., **A**) and resting (i.e., $\mathbf{5_{cyc}}$) states that strongly favored the latter.

Collectively, the experiments investigating the behavior of open catalysts $\mathbf{5_{acyc}}$ – $\mathbf{7_{acyc}}$ revealed that controlling the tether lengths of cyclic catalysts may dictate polymerization kinetics with regard to polymer MWs and polydispersities. For example, shorter tether lengths may facilitate catalyst release during polymerization (Scheme 1), ultimately leading to multiple macrocycles produced from each catalyst molecule. Alternatively, REMP catalysts displaying little tendency to be released from a cyclic polymer may provide access to cyclic block copolymers or other advanced macrocycles.

Interaction Between Free Catalyst and Polymer

As mentioned previously, it may be possible for a cyclic catalyst to equilibrate with poly(olefin)s and become incorporated (or reincorporated) into a polymer chain. This equilibrium, depicted in Scheme 5, may be tether length-dependent given that ring-opening of the catalyst may be a driving force toward incorporation into the polymer. With regard to REMP, the reversibility of intramolecular chain-transfer and catalyst release (Scheme 1) would result in an equilibrium amount of Ru species contained within the final cyclic polymers. Therefore, understanding each catalyst's affinity toward polymer incorporation is important for understanding the potential purity of the cyclic polymers. To investigate, we prepared linear PCOE via ROMP using acyclic catalyst **3** in the presence of 3-hexene as a chain-transfer agent. This provided a hydrocarbon polymer (M_n = 150 kDa, PDI = 2.1) which closely resembled the PCOE obtained via REMP in composition.[33] The linear PCOE was then treated with each of the cyclic catalysts $\mathbf{5_{cyc}}-\mathbf{7_{cyc}}$ (olefin/catalyst molar ratio = 100:1) in CD_2Cl_2 at 40 °C. The equilibration of catalyst and polymer was monitored via ^{1}H NMR spectroscopy using anthracene as an internal standard; key NMR signals of the cyclic catalysts and incorporated species were similar to those observed in the previous section (Scheme 4).

As expected, incorporation of cyclic catalyst into the polymer chain was dependent on the tether length of the catalyst. Specifically, after 1 h ca 11% of catalyst $\mathbf{7_{cyc}}$ had become incorporated into the polymer, whereas catalyst $\mathbf{6_{cyc}}$ showed only 3% incorporation over the same time period. Catalyst $\mathbf{5_{cyc}}$, however, revealed no incorporation even after extended periods (up to 6 h). To compare, catalyst $\mathbf{5_{cyc}}\cdot\mathbf{H_2}$ was also studied and gave similar results as $\mathbf{5_{cyc}}$. Overall, although the amount of incorporated catalyst was small in each case, there appeared to be some equilibration of free catalyst into the poly(olefin) depending upon the length of the catalyst tether. Notably, equilibration appeared to be slow in comparison with polymerization data presented above. Therefore, avoiding prolonged polymerization reaction times may be sufficient for minimizing the amount of Ru in the resulting polymers.

Conclusions

In summary, we describe the synthesis and characterization of a series of cyclic Ru-alkylidene catalysts with particular focus on their ability to mediate ring-expansion metathesis polymerization. Both catalyst tether length as well as NHC electronics were found to significantly impact different aspects of the polymerization mechanism. Whereas shorter tether lengths were more efficient for catalyst release from the polymer, the caveat for these systems was found to be slower polymerization rates. Saturation of the NHC backbone, however, increased polymerization efficiency and effectively balanced activity loss due to shortening of the tether. Overall, catalyst stabilities were found to be good over the course of the polymerization experiments. The ability to control catalyst activity by a combination of tether length and ligand electronics may lead to new opportunities in olefin metathesis and catalyst design.

Experimental Section

Materials and Methods

^{1}H and ^{13}C NMR spectra were recorded using a Varian Mercury 300 or Varian Inova 500 spectrometer and were routinely run using broadband decoupling. Chemical shifts (δ) are expressed in ppm downfield from tetramethylsilane using the residual protiated solvent as an internal standard ($CDCl_3$ ^{1}H: 7.26 ppm and ^{13}C: 77.0 ppm; C_6D_6 ^{1}H: 7.20 ppm and ^{13}C: 128.0 ppm). ^{31}P NMR spectra were externally referenced to 85% H_3PO_4 (0.00 ppm). Coupling constants are expressed in hertz (Hz). THF, CH_2Cl_2, Et_2O, pentane, PhH, $PhCH_3$, and C_6D_6 were obtained from solvent purification columns.[34] CD_2Cl_2 used for NMR-scale experiments

was distilled over CaH_2 under N_2 prior to use. $CHCl_3$ was distilled over P_2O_5 under N_2 prior to use. Ru-complex **1** was obtained from Materia, Inc. All other solvents and reagents were of reagent quality and used as obtained from commercial sources. Chromatography was performed with neutral silica gel (TSI Scientific, 230–400mesh, pH 6.5 – 7.0). Crystallographic data have been deposited at the CCDC, 12 Union Road, Cambridge CB2 1EZ, U.K., and copies can be obtained on request, free of charge, by quoting the publication citation and the deposition numbers 687290 ($\mathbf{5_{cyc}}\cdot\mathbf{H_2}$), 683585 ($\mathbf{6_{cyc}}$), and 687247 ($\mathbf{6_{cyc}}\cdot\mathbf{H_2}$).

Cyclic complex $\mathbf{5_{cyc}}\cdot\mathbf{H_2}$

In a Schlenk tube, chloroform adduct **11a** (200 mg, 0.51 mmol) was dissolved in dry THF (515 mL) under at atmosphere of dry N_2. To the solution was added Ru-complex **1** (210 mg, 0.26 mmol). The flask was sealed and the reaction mixture was stirred in an oil bath at 70 °C for 2 h. Afterward, the cooled reaction mixture was concentrated under vacuum, redissolved in a minimal amount of PhH, and treated dropwise with pentane until crystallization ensued (X-ray analysis was performed on crystals obtained in this manner). The solids were collected by vacuum filtration, rinsed with 5% Et_2O/pentane, and dried under vacuum to provide 147 mg (81% yield) of the desired complex as a tan solid. ^{1}H NMR (500 MHz, C_6D_6): δ 20.39 (dt, $3J_{H,P}$ = 9.3 Hz, $J_{H,H}$ = 4.5 Hz, 1H), 6.93 (s, 2H), 3.17 (t, J = 10.0 Hz, 2H), 3.10-3.09 (m, 2H), 2.85 (t, J = 10.0 Hz, 2H), 2.75 (br, 2H), 3.71 (s, 6H), 2.60-2.53 (m, 3H), 2.32 (br 2H), 2.23 (s, 3H), 1.95-1.92 (m, 6H), 1.78 (br, 6H), 1.68 (br, 2H), 1.47-1.45 (m, 6H), 1.34-1.29 (m, 10H), 1.19-1.17 (m, 2H). ^{13}C NMR (125 MHz, C_6D_6): δ 216.0 (J_{CP} = 85.9 Hz), 138.4, 137.6, 136.6, 129.9, 57.9 (J_{CP} = 4.9 Hz), 51.2 (J_{CP} = 3.5 Hz), 48.5 (J_{CP} = 2.7 Hz), 47.9, 32.1 (J_{CP} = 15.1 Hz), 29.8, 28.2 (J_{CP} = 10.4 Hz), 27.3, 26.8, 26.7, 21.1, 20.0. ^{31}P NMR (121 MHz, C_6D_6): δ 27.0. HRMS m/z calcd for $C_{35}H_{57}Cl_2N_2PRu$ [M^+] 708.2680, found 708.2659.

[1-(6-Heptenyl)-3-mesitylimidazolylidene]$RuCl_2$(=CHPh) (PCy_3) ($\mathbf{6_{acyc}}$)

Imidazolium bromide $\mathbf{8_{n=5}}$ (400 mg, 1.10 mmol), was suspended in dry $PhCH_3$ (7 mL) under dry N_2. To the solution was added NaOtBu (106 mg, 1.10 mmol) and the resulting mixture was stirred at RT for 12 h. Ru-complex **1** (453 mg, 0.55 mmol) was then added in a single portion and the resulting mixture was stirred for 1 h during which time a color change from purple to brown was observed. Upon completion, the mixture was filtered through a thin pad of TSI silica gel using Et_2O/pentane (1:4 v/v) as eluent. The filtrate was concentrated under vacuum without heating. Purification by column chromatography on TSI silica gel under N_2 pressure (10% Et_2O/pentane) provided 408 mg (90% yield) of the desired compound as a red-purple powder. ^{1}H NMR (major isomer) (300 MHz, C_6D_6): δ 19.85 (s, 1H), 7.05-6.94 (m, 2H) 6.56-6.55 (m, 1H), 6.31-6.15 (m, 3H), 5.90-5.76 (m, 1H), 5.15-5.03 (m, 2H), 4.70 (t, J = 7.7 Hz, 2H), 2.65-2.53 (m, 4H), 2.13 (s, 3H), 1.97-1.08 (m, 37H), 1.80 (s, 6H). ^{31}P NMR (major isomer) (121 MHz, C_6D_6): δ 34.4. HRMS m/z calcd for $C_{44}H_{65}Cl_2N_2PRu$ [M^+] 824.3306, found 824.3298.

Cyclic complex $\mathbf{6_{cyc}}$

Ru-complex $\mathbf{6_{acyc}}$ (400 mg, 0.48 mmol), was dissolved in dry PhH (30 mL) and pentane (450 mL) in a Schlenk tube under dry N_2. The mixture was then placed in a oil bath at 70 °C and stirred for 1 h. Upon completion, the solution was cooled to RT, transferred to a round-bottom flask, and concentrated under vacuum without heat. The crude material was triturated with 20% Et_2O/pentane (50 mL) for ca 20 min. The solids were then collected via vacuum filtration, rinsed with pentane, and dried under vacuum to provide 335 mg (96% yield) of the desired compound as a red-brown powder. X-ray quality crystals were obtained by slow addition of pentane to a PhH solution of the complex. ^{1}H NMR (300 MHz, C_6D_6): δ 19.71 (dt, $3J_{H,P}$ = 5.1 Hz, $J_{H,H}$ = 5.5 Hz, 1H), 6.90 (s, 2H), 6.35 (d, J = 1.8 Hz, 1H), 6.14 (s, 1H), 2.74-2.51 (m, 3H), 2.51 (s, 6H), 2.23 (s, 3H), 1.99-1.31 (m, 40H). ^{13}C NMR (125 MHz, C_6D_6): δ 186.0

(J_{CP} = 84.7 Hz), 138.2, 137.1, 129.4, 128.3, 123.6 (J_{CP} = 2.3 Hz), 120.4, 62.9, 47.0, 32.4 (J_{CP} = 16.9 Hz), 31.5, 29.8, 28.1 (J_{CP} = 10.0 Hz), 26.8, 22.9, 21.1, 19.7. ^{31}P NMR (121 MHz, C_6D_6): δ 33.3. HRMS m/z calcd for $C_{36}H_{57}Cl_2N_2PRu$ [M^+] 720.2680, found 720.2671.

Cyclic complex 6_{cyc}·H_2

This compound was prepared analogously to **5_{cyc}·H_2** from chloroform adduct **11b** (280 mg, 0.69 mmol) and Ru-complex **1** (285 mg, 0.35 mmol) in THF (650 mL) to provide 369 mg (74% yield) of the desired complex as a red-brown solid. X-ray quality crystals were obtained by slow diffusion of pentane into a Et_2O/PhH (20:1 v/v) solution of the complex. ^{1}H NMR (500 MHz, C_6D_6): δ 19.61 (dt, $3J_{H,P}$ = 5.0 Hz, $J_{H,H}$ = 5.7 Hz, 1H), 6.93 (s, 2H), 3.33-2.83 (m, 4H), 2.70 (s, 6H), 2.63-2.56 (m, 3H), 2.22 (s, 3H), 1.93-1.30 (m, 40H). ^{13}C NMR (125 MHz, C_6D_6): δ 215.3 (J_{CP} = 80.1 Hz) 137.5, 137.0, 129.9, 129.5, 62.8, 51.7 (J_{CP} = 3.3 Hz), 47.7, 46.9, 32.2 (J_{CP} = 16.5 Hz), 29.7, 28.1 (J_{CP} = 10.1 Hz), 27.9, 26.8, 25.6, 23.6, 21.1. ^{31}P NMR (121 MHz, C_6D_6): δ 30.4. HRMS m/z calcd for $C_{36}H_{59}Cl_2N_2PRu$ [M^+] 722.2837, found 722.2808.

Cyclic complex 7_{cyc}

This compound was prepared analogously to **6_{cyc}** from open complex **7_{acyc}** (150 mg, 0.18 mmol) in PhH (10 mL) and pentane (170 mL). Upon completion, the cooled reaction mixture was concentrated under vacuum without heat, then triturated with 20% Et_2O/pentane (10 mL) for ca 20 min. The solids were collected via vacuum filtration and further purification via column chromatography on TSI silica gel under N_2 pressure (30% Et_2O/pentane) provided 56 mg (42% yield) of the desired compound as a light brown powder. ^{1}H NMR (500 MHz, C_6D_6): δ 19.37 (dt, $3J_{H,P}$ = 10.2 Hz, $J_{H,H}$ = 5.5 Hz, 1H), 6.92 (s, 2H), 6.38 (d, J = 1.5 Hz, 1H), 6.19 (s, 1H), 3.66 (br, 2H), 2.62-2.57 (m, 3H), 2.54 (s, 6H), 2.24 (s, 3H), 2.08-1.61 (m, 24H), 1.50-1.42 (m, 2H), 1.34-1.28 (m, 12H), 1.22-1.17 (m, 2H). ^{13}C NMR (125 MHz, C_6D_6): δ 184.7 (J_{CP} = 97.5 Hz), 138.1, 137.6, 129.2, 128.4, 128.3, 128.1, 127.9, 123.3 (J_{CP} = 3.3 Hz), 119.9, 60.4, 47.1, 32.7 (J_{CP} = 16.1 Hz), 29.9, 28.2 (J_{CP} = 9.5 Hz), 26.8, 26.5, 24.7, 21.1, 20.7, 19.7. ^{31}P NMR (121 MHz, C_6D_6): δ 26.3. HRMS m/z calcd for $C_{37}H_{59}Cl_2N_2PRu$ [M^+] 734.2837, found 734.2814.

1-(6-Heptenyl)-3-mesitylimidazolium bromide ($8_{n=5}$)

This compound was prepared analogously to **$8_{n=3,4,6}$** from *N*-mesitylimidazole (1.00 g, 5.37 mmol) and 7-bromo-1-heptene (1.0 mL, 6.55 mmol) in $PhCH_3$ (20 mL).[9] Upon completion, the reaction mixture was concentrated under vacuum and the crude material was suspended in Et_2O (100 mL) and vigorously stirred for 12 h to produce a fine white suspension. The solids were collected via vacuum filtration under a stream a N_2 to provide 1.81 g (93% yield) of the desired compound as an off-white powder.[35] ^{1}H NMR (300 MHz, $CDCl_3$): δ 10.31 (dd appearing as t, J = 1.5 Hz, 1H), 7.94 (dd apearing as t, J = 1.7 Hz, 1H), 7.21 (dd apearing as t, J = 1.7 Hz, 1H), 6.94 (s, 2H), 5.76-5.63 (m, 1H), 4.96-4.84 (m, 2H), 4.67 (t, J = 7.4 Hz, 2H), 2.29 (s, 3H), 2.01 (s, 6H), 2.01-1.91 (m, 4H), 1.43-1.30 (m, 4H). ^{13}C NMR (125 MHz, $CDCl_3$): δ 141.1, 138.1, 137.8, 134.0, 130.6, 129.7, 123.2, 123.1, 114.7, 50.1, 33.2, 30.2, 28.0, 25.3, 21.0, 17.5. HRMS m/z calcd for $C_{19}H_{27}N_2$ [M^+] 283.2174, found 283.2186.

1-(5-Hexenyl)-3-mesitylimidazolinium bromide (10a)

To a solution of $HC(OEt)_3$ (10 mL) and $PhCH_3$ (10 mL) in a 50 mL round-bottom flask was added PTSA·H_2O (39 mg, 0.20 mmol), *N*-mesitylethylenediamine (**9**) (729 mg, 4.09 mmol), and 6-bromo-1-hexene (0.66 mL, 4.91 mmol). The flask was fitted with a H_2O-jacketed condenser and the reaction mixture was stirred under N_2 in an oil bath at 110 °C for 10 h. Afterward, the cooled reation mixture was concentrated under vacuum. The crude product was treated with Et_2O (40 mL) and vigorously stirred for 2 h to produce an off-white slurry. The

solids were collected via vacuum filtration, rinsed with Et_2O, and dried under vacuum to provide 1.31 g (91% yield) of the desired compound. ^{1}H NMR (300 MHz, $CDCl_3$): δ 9.50 (s, 1H), 6.87 (s, 2H), 5.80-5.67 (m, 1H), 5.03-4.92 (m, 2H), 4.30-4.11 (m, 4H), 3.94 (t, *J* = 7.2 Hz, 2H), 2.26 (s, 6H), 2.24 (s, 3H), 2.12-2.05 (m, 2H), 1.76-1.66 (m, 2H), 1.49-1.42 (m, 2H). ^{13}C NMR (125 MHz, $CDCl_3$): δ 158.7, 139.9, 137.6, 135.0, 130.4, 129.7, 115.2, 50.9, 48.7, 48.1, 32.8, 26.4, 25.2, 20.8, 17.9. HRMS m/z calcd for $C_{18}H_{27}N_2$ [M^+] 271.2174, found 271.2161.

1-(6-Heptenyl)-3-mesitylimidazolinium bromide (10b)

This compound was prepared analogously to **10a** from $HC(OEt)_3$ (7.0 mL), $PhCH_3$ (7.0 mL), PTSA·H_2O (27 mg, 0.14 mmol), *N*-mesitylethylenediamine (**9**) (500 mg, 2.80 mmol), and 7-bromo-1-heptene (0.51 mL, 3.36 mmol) to provide 951 mg (93% yield) of the desired compound. ^{1}H NMR (500 MHz, $CDCl_3$): δ 9.31 (s, 1H), 6.77 (s, 2H), 5.70-5.61 (m, 1H), 4.90-4.81 (m, 2H), 4.20-4.16 (m, 2H), 4.12-4.08 (m, 2H), 3.78 (t, *J* = 7.3 Hz, 2H), 2.16 (s, 3H), 2.15 (s, 6H), 1.96-1.91 (m, 2H), 1.64-1.58 (m, 2H), 1.35-1.30 (m, 2H), 1.27-1.21 (m, 2H). ^{13}C NMR (125 MHz, $CDCl_3$): δ 158.5, 139.7, 138.1, 134.9, 130.3, 129.5, 114.4, 50.8, 48.6, 48.0, 33.1, 27.9, 26.7, 25.3, 20.7, 17.8. HRMS m/z calcd for $C_{19}H_{29}N_2$ [M^+] 285.2325, found 285.2310.

1-(5-Hexenyl)-3-mesityl-2-(trichloromethyl)imidazolidine (11a)

Under an atmosphere of dry N_2, imidazolinium bromide **10a** (443 mg, 1.26 mmol) was dissolved in dry $CHCl_3$ (6 mL). NaH (95 wt%, 38 mg, 1.51 mmol) was then added portionwise under a stream of N_2. The resulting mixture was placed in an oil bath at 55 °C and stirred for 10 h. Afterward, the cooled reaction mixture was diluted with Et_2O (100 mL), filtered through a thin pad of silica gel, and concentrated to provide 305 mg (62% yield) of the desired product as a pale yellow oil. ^{1}H NMR (300 MHz, $CDCl_3$): δ 6.86 (s, 1H), 6.85 (s, 1H), 5.91-5.78 (m, 1H), 5.07-4.95 (m, 2H), 4.73 (s, 1H), 3.86-3.78 (m, 1H), 3.62-3.55 (m, 1H), 3.41-3.32 (m, 1H), 3.23-3.16 (m, 1H), 3.10-3.02 (m, 1H), 2.98-2.90 (m, 1H), 2.35 (s, 3H), 2.70 (s, 3H), 2.25 (s, 3H), 2.16-2.09 (m, 2H), 1.68-1.43 (m, 4H). ^{13}C NMR (75 MHz, $CDCl_3$): δ 147.8, 147.7, 142.8, 138.8, 138.7, 134.9, 132.6, 129.9, 129.5, 114.5, 108.2, 94.2, 58.2, 52.9, 52.6, 33.7, 29.7, 26.1, 20.7, 19.8, 19.3. HRMS m/z calcd for $C_{19}H_{27}Cl_3N_2$ [M^+] 388.1240, found 388.1225.

1-(6-Heptenyl)-3-mesityl-2-(trichloromethyl)imidazolidine (11b)

This compound was prepared analogously to **11a** from imidazolinium bromide **10b** (730 mg, 2.0 mmol), $CHCl_3$ (8 mL), and NaH (95 wt%, 101 mg, 4.00 mmol) to provide 670 mg (83% yield) of the desired product as a pale yellow oil. ^{1}H NMR (300 MHz, $CDCl_3$): δ 6.88 (s, 1H), 6.86 (s, 1H), 5.92-5.79 (m, 1H), 5.08-4.96 (m, 2H), 4.75 (2, 1H), 3.87-3.80 (m, 1H), 3.65-3.58 (m, 1H), 3.42-3.33 (m, 1H), 3.25-3.17 (m, 1H), 3.10-3.02 (m, 1H), 3.00-2.92 (m, 1H), 2.37 (s, 3H), 2.29 (s, 3H), 2.27 (s, 3H), 2.14-2.05 (m, 2H), 1.68-1.54 (m, 2H), 1.50-1.38 (m, 4H). ^{13}C NMR (75 MHz, $CDCl_3$): δ 142.8, 139.0, 138.6, 134.8, 132.6, 129.9, 129.4, 114.3, 108.2, 94.2, 58.4, 52.9, 52.6, 33.8, 30.1, 28.8, 26.4, 20.7, 19.8, 19.3. HRMS m/z calcd for $C_{20}H_{29}Cl_3N_2$ [M^+] 402.1396, found 402.1382.

Supplementary Material

Refer to Web version on PubMed Central for supplementary material.

Acknowledgements

We gratefully acknowledge Materia, Inc. for the generous gift of catalyst **1**. We thank the DoE (DE-FG02-05ER46218) and the California Institute of Technology for generous financial support. AJB thanks the NIH/NCI for a postdoctoral

fellowship. We thank Professor Gregory B. McKenna for helpful discussions, as well as Matthew T. Whited, Larry M. Henling, and Dr. Michael W. Day for help in obtaining X-ray data.

References

1. For general reviews on Ru-catalyzed olefin metathesis, see: (a) Bielawski CW, Grubbs RH. Prog Polym Sci 2007;32:1–29. (b) Grubbs RH. Tetrahedron 2004;60:7117.(c)GrubbsRHHandbook of MetathesisWiley-VHCWeinheim, Germany2003 (d) Trkna TM, Grubbs RH. Acc Chem Res 2001;34:18. [PubMed: 11170353] (e) Grubbs RH, Chang S. Tetrahedron 1998;54:4413.(f) IvinKJMolJCOlefin Metathesis and Metathesis PolymerizationAcademic PressSan Diego, CA1997
2. (a) Xia Y, Verduzco R, Grubbs RH, Kornfield JA. J Am Chem Soc 2008;130:1735. [PubMed: 18197667] (b) Gorodetskaya IA, Choi TL, Grubbs RH. J Am Chem Soc 2007;129:12672. [PubMed: 17902678] (c) Choi TL, Rutenberg IM, Grubbs RH. Angew Chem Int Ed 2002;41:3839.
3. (a) Copéret C, Basset JM. Adv Synth Catal 2007;349:78. (b) Colacino E, Martinez J, Lamaty F. Coord Chem Rev 2007;251:726.
4. (a) Funk TW, Berlin JM, Grubbs RH. J Am Chem Soc 2006;128:1840. [PubMed: 16464082] (b) Berlin JM, Goldberg SD, Grubbs RH. Angew Chem Int Ed 2006;45:7591.
5. (a) Louie J, Bielawski CW, Grubbs RH. J Am Chem Soc 2001;123:11312. [PubMed: 11697983] (b) Bielawski CW, Louie J, Grubbs RH. J Am Chem Soc 2000;122:12872.
6. (a) Choi TL, Grubbs RH. Angew Chem Int Ed 2003;42:1743. (b) Love JA, Morgan JP, Trnka TM, Grubbs RH. Angew Chem Int Ed 2002;41:4035.
7. (a) Matloka PP, Wagener KB. J Mol Catal A: Chem 2006;257:89. (b) Baughman TW, Wagener KB. Adv Polym Sci 2005;176:1. (c) Schwendeman JE, Church AC, Wagener KB. Adv Synth Catal 2002;344:597.
8. (a) Vougioukalakis GC, Grubbs RH. J Am Chem Soc 2008;130:2234. [PubMed: 18220390] (b) Plietker B, Neisius NM. J Org Chem 2008;73:3218. [PubMed: 18358049] (c) Vougioukalakis GC, Grubbs RH. Organometallics 2007;26:2469. (d) Vehlow K, Maechling S, Blechert S. Organometallics 2006;25:25. (e) Hansen EC, Lee D. Org Lett 2004;6:2035. [PubMed: 15176812] (f) Chatterjee AK, Choi TL, Sanders DP, Grubbs RH. J Am Chem Soc 2003;125:11360. [PubMed: 16220959]
9. For the synthesis and structural characterization of 4_{cyc} and 5_{cyc}, see: Fürstner A, Ackermann L, Gabor B, Goddard R, Lehmann CW, Mynott R, Stelzer F, Thiel OR. Chem Eur J 2001;7:3236.
10. Here we use the subscript “cyc” to denote the “cyclic” catalysts, and the subscript “acyc” to denote the pre-cyclized, acyclic complexes.
11. (a) Bielawski CW, Benitez D, Grubbs RH. J Am Chem Soc 2003;125:8424. [PubMed: 12848534] (b) Bielawski CW, Benitez D, Grubbs RH. Science 2002;297:2041. [PubMed: 12242440]
12. For additional cyclic polymer syntheses involving ring-expansion approaches, see: (a) Culkin, Darcy A.; Jeong, Wonhee; Csihony, Szilárd; Gomez, Enrique D.; Balsara, Nitash P.; Hedrick, James L.; Waymouth, Robert M. Angew Chem Int Ed 2007;46:2627. (b) Li H, Debuigne A, Jérome R, Lecomte P. Angew Chem Int Ed 2006;45:2264. (c) He T, Zheng GH, Pan CY. Macromolecules 2003;36:5960. (d) Kudo H, Makino S, Kameyama A, Nishikubo T. Macromolecules 2005;38:5964. (e) Shea KJ, Lee SY, Busch BB. J Org Chem 1998;63:5746. [PubMed: 11672170]
13. For cyclic polymer syntheses involving ring-closing of telechelic polymers, see: (a) Schappacher M, Deffieux A. Science 2008;319:1512. [PubMed: 18339934] (b) Laurent BA, Grayson SM. J Am Chem Soc 2006;128:4238. [PubMed: 16568993] (c) Oike H, Mouri T, Tezuka Y. Macromolecules 2001;34:6229. (d) Alberty KA, Tillman E, Carlotti S, Bradforth SE, Hogen-Esch TE, Parker D, Feast WJ. Macromolecules 2002;35:3856. (e) Roovers J. J Polym Sci, Part B: Polym Phys 1988;26:1251. (f) Roovers J, Toporowski PM. Macromolecules 1983;16:843. (g) Geiser D, Hoeker H. Macromolecules 1980;13:653.
14. (a) Sanford MS, Love JA, Grubbs RH. J Am Chem Soc 2001;123:6543. [PubMed: 11439041] (b) Bielawski CW, Grubbs RH. Angew Chem Int Ed 2000;39:2903.
15. See Supporting Information.
16. In solution, complexes $4_{acyc} - 7_{acyc}$ appeared to exist as a mixture of two rotamers as shown by two benzylidene signals (ratio ca 10:1). The major isomer appeared as a singlet, analogous to complex 2, whereas a second signal was observed further downfield as a doublet (e.g., $^{3}J_{H,P}$ = 12.9 Hz for 6_{cyc}).[15]

17. Purchased from TSI Scientific, 230–400 mesh, neutral pH.
18. Notably, “open” complexes $4_{acyc} - 7_{acyc}$ were routinely used in subsequent cyclization steps following only filtration through a short silica gel plug and concentration under vacuum. Residual tricyclohexylphosphine was efficiently removed from the cyclized catalysts ($4_{cyc} - 7_{cyc}$) during purification.
19. Additional considerations should be noted: 1) intramolecular cyclization may proceed to directly give an acyclic methylidene complex that is identical to the product that would be obtained between CM of styrene and the cyclic catalyst, and 2) in rare cases, olefin isomerization and cyclization to give small amounts of cyclic catalysts bearing a one-carbon shorter tether were observed (e.g., $7_{acyc} \rightarrow 6_{cyc}$).
20. Perillo I, Caterina MC, López J, Salerno A. Synthesis 2004:851.
21. For an alternative, two-step procedure for the synthesis of imidazolinium salts bearing one *N*-aryl and one *N*′-alkyl group, see ref 8d.
22. Attempts at ligand exchange via deprotonation of imidazolinium salts 10 in hexanes were also unsuccessful.
23. (a) Courchey FC, Sworen JC, Ghiviriga I, Abboud KA, Wagener KB. Organometallics 2006;25:6074. (b) Trnka TM, Morgan JP, Sanford MS, Wilhem TE, Scholl M, Choi TL, Ding S, Day MD, Grubbs RH. J Am Chem Soc 2003;125:2546. [PubMed: 12603143]
24. This reaction was found to be solvent-dependent and $PhCH_3$, PhH, pentane, and PhH/pentane mixture gave inferior results.
25. Unfortunately, attempts to isolate pure samples of $7_{cyc}{\cdot}H_2$ were unsuccessful.
26. Attempts to obtain X-ray quality crystals of 7_{cyc} were met with limited success.
27. Since single-crystal X-ray data was not obtained for 7_{cyc}, therefore, it was not possible to determine the direction of the rotation about the Ru1-C2 bond with respect to complexes $4_{cyc} - 6_{cyc}$. We speculate that the long tether of 7_{cyc} may allow for conformations that collectively frustrate crystallization.
28. Additional representations of the data in Figure 4 are provided.[15]
29. Ritter T, Hejl A, Wenzel AG, Funk TW, Grubbs RH. Organometallics 2006;25:5740.
30. Other terminating agents have also been employed, see: (a) Matson, J. B.; Grubbs, R. H. Macromolecules 2008, in press (DOI: 10.1021/ma800980p). (b) Hilf S, Berger-Nicoletti E, Grubbs RH, Kilbinger AFM. Angew Chem Int Ed 2006;45:8045. (c) Owen RM, Gestwicki JE, Young T, Kiessling LL. Org Lett 2002;4:2293. [PubMed: 12098230]
31. In light of the relatively low activity of 4_{cyc}, 4_{acyc} was not evaluated in these experiments.
32. Under identical conditions, $5_{acyc} - 7_{acyc}$ gave faster conversions of COE to PCOE than the corresponding “closed” systems ($5_{cyc} - 7_{cyc}$). The higher polymerization activities of $5_{acyc} - 7_{acyc}$ versus $5_{cyc} - 7_{cyc}$ may reflect restricted conformations of the latter. Further investigations are underway.
33. Molecular-weight data was obtained from triple-angle laser light-scattering and refractive index measurements.
34. Pangborn AB, Giardello MA, Grubbs RH, Rosen RK, Timmers FJ. Organometallics 1996;15:1518–1520.
35. The compound appeared to be hygroscopic, producing a thick, viscous material when collected under air.

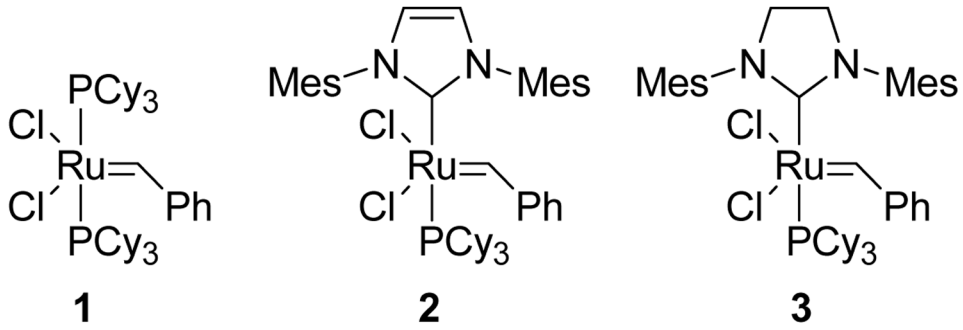

Figure 1.
Representative Ru-based metathesis catalysts.

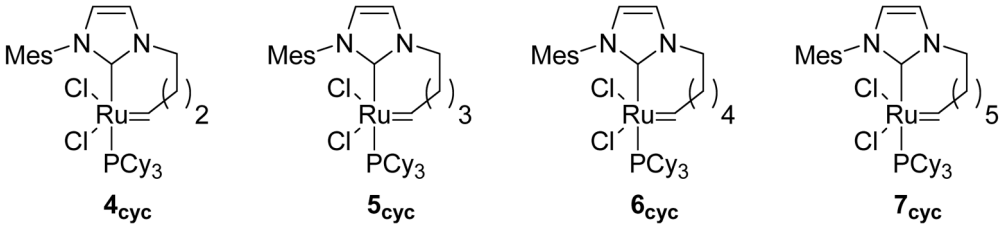

4cyc **5cyc** **6cyc** **7cyc**

Figure 2.
Cyclic Ru-alkylidene metathesis catalysts.

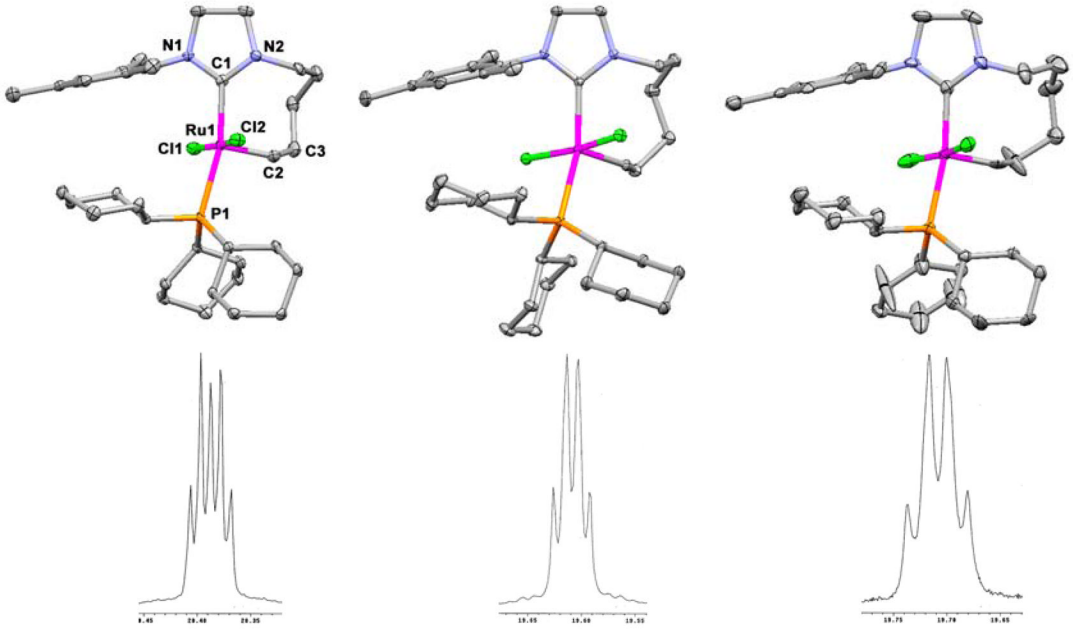

Figure 3.
(top): X-ray crystal structures of $\mathbf{5_{cyc}}\cdot\mathbf{H_2}$, $\mathbf{6_{cyc}}$, and $\mathbf{6_{cyc}}\cdot\mathbf{H_2}$. Solvent molecules and hydrogens have been removed for clarity. Ellipsoids are drawn at the 50% probability level.
(bottom): ^{1}H NMR spectra (C_6D_6) of alkylidene proton of $\mathbf{5_{cyc}}\cdot\mathbf{H_2}$, $\mathbf{6_{cyc}}$, and $\mathbf{6_{cyc}}\cdot\mathbf{H_2}$.

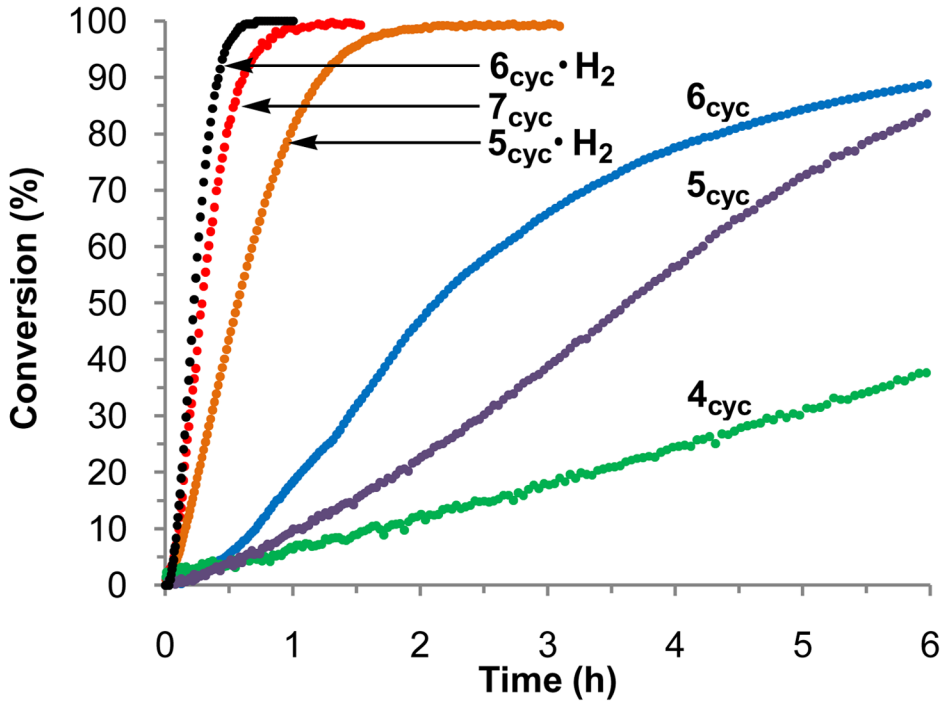

Figure 4.
REMP of COE using catalysts **4**$_{cyc}$ (green), **5**$_{cyc}$ (purple), **5**$_{cyc}$·**H**$_2$ (orange), **6**$_{cyc}$ (blue), **6**$_{cyc}$·**H**$_2$ (black), and **7**$_{cyc}$ (red). Conditions: CD_2Cl_2, 40 °C, $[M/C]_0$ = 1000:1, $[M]_0$ = 0.5 M. Conversion determined by ^{1}H NMR spectroscopy.

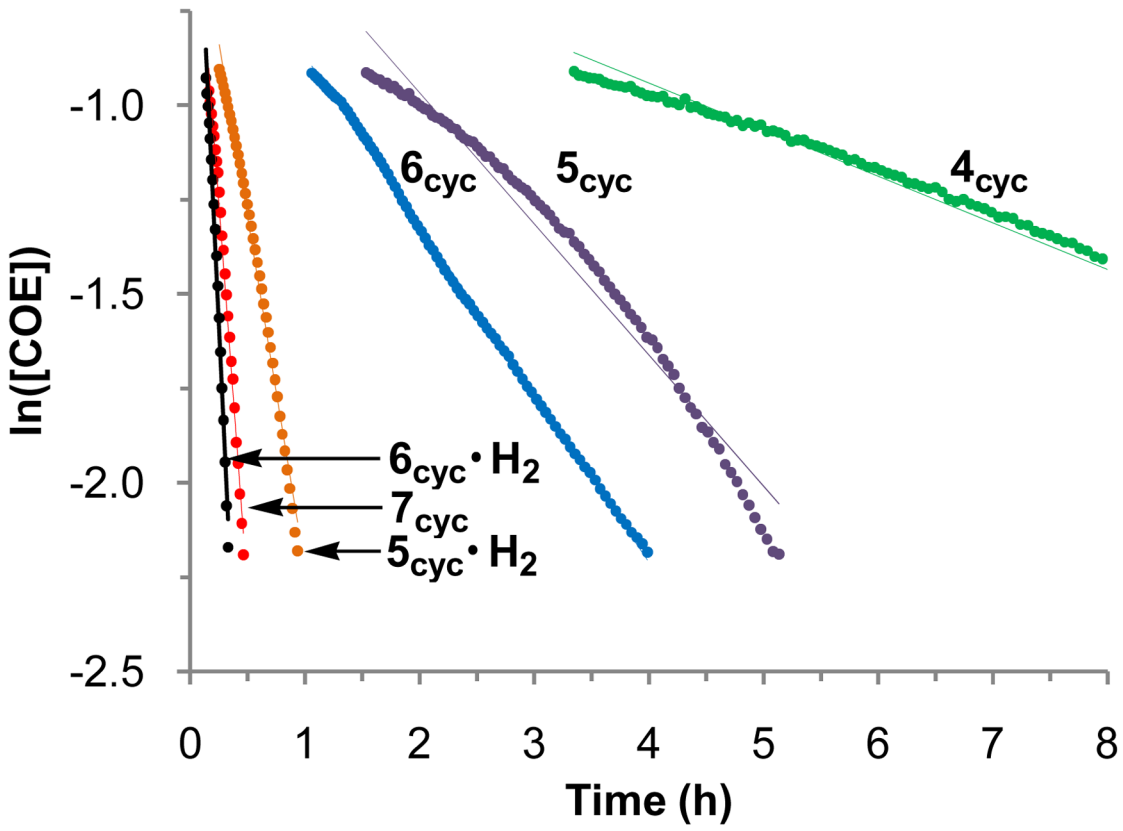

Figure 5.
Log plots for REMP of COE using catalysts $\mathbf{4_{cyc}}$ (green), $\mathbf{5_{cyc}}$ (purple), $\mathbf{5_{cyc}}\cdot\mathbf{H_2}$ (orange), $\mathbf{6_{cyc}}$ (blue), $\mathbf{6_{cyc}}\cdot\mathbf{H_2}$ (black), and $\mathbf{7_{cyc}}$ (red). Linear least-squares fitting gave R^2 values of: $\mathbf{4_{cyc}}$, 0.997; $\mathbf{5_{cyc}}$, 0.969; $\mathbf{5}_{\mathbf{cyc}}\cdot\mathbf{H_2}$, 0.991; $\mathbf{6_{cyc}}$, 0.998; $\mathbf{6_{cyc}}\cdot\mathbf{H_2}$, 0.990; and $\mathbf{7_{cyc}}$, 0.991. Conditions: CD_2Cl_2, 40 °C, $[M/C]_0$ = 1000:1, $[M]_0$ = 0.5 M. Data recorded using ^1H NMR spectroscopy.

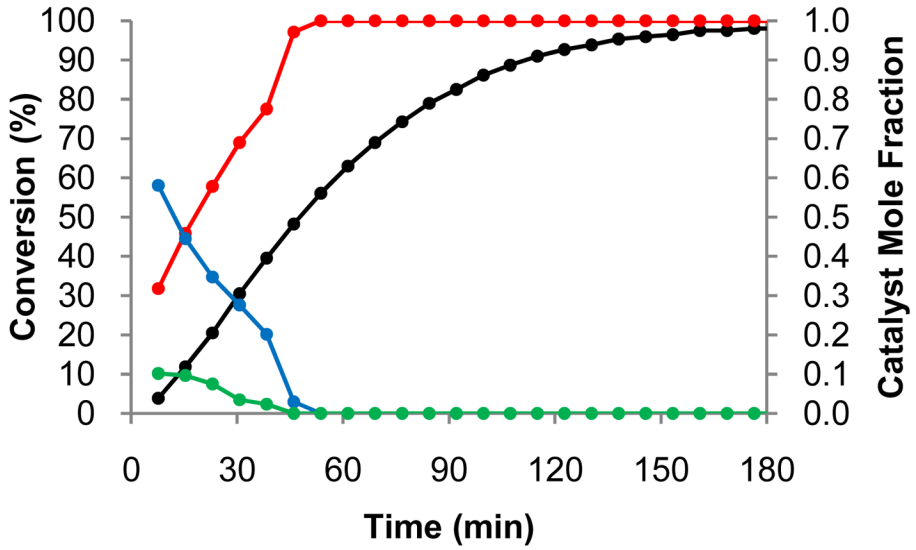

Figure 6.

Left axis: Conversion of COE to PCOE using $\mathbf{5}_{\mathbf{acyc}}$ (black). Right axis: Mole fraction of $\mathbf{5}_{\mathbf{cyc}}$ (red), $\mathbf{5}_{\mathbf{acyc}}$ (blue), and **A** (green). Conditions: CD_2Cl_2, 40 °C, $[COE/\mathbf{5}_{\mathbf{acyc}}]_0$ = 250:1, $[COE]_0$ = 0.5 M. Conversion determined by ^1H NMR spectroscopy.

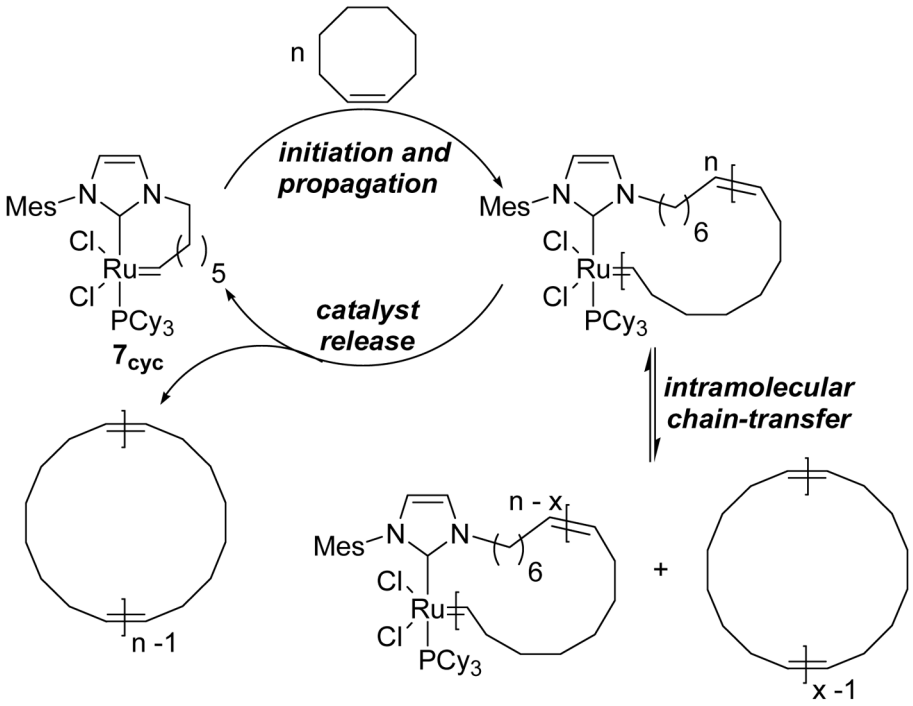

Scheme 1.
Proposed REMP catalytic cycle.

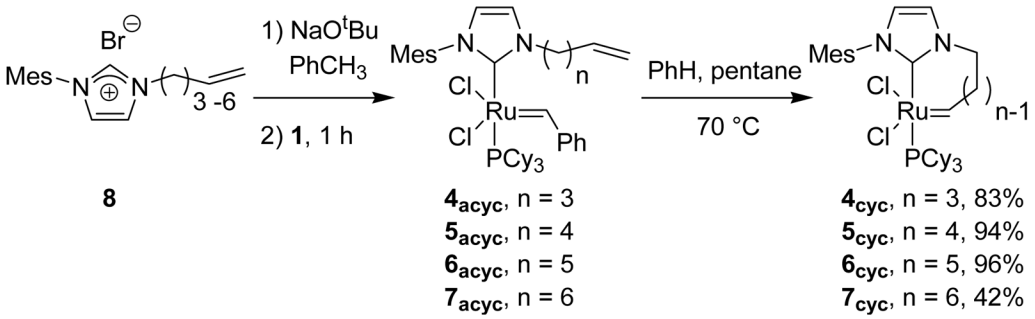

8

4$_{acyc}$, n = 3
5$_{acyc}$, n = 4
6$_{acyc}$, n = 5
7$_{acyc}$, n = 6

4$_{cyc}$, n = 3, 83%
5$_{cyc}$, n = 4, 94%
6$_{cyc}$, n = 5, 96%
7$_{cyc}$, n = 6, 42%

Scheme 2.
Synthesis of cyclic REMP catalysts **4**$_{cyc}$ – **7**$_{cyc}$.

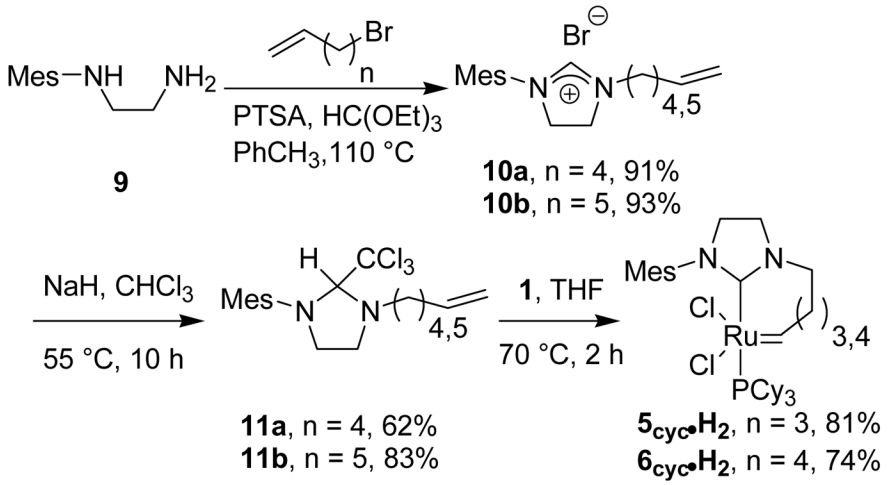

Scheme 3.
Synthesis of "saturated" catalysts $\mathbf{5_{cyc}}\cdot\mathbf{H_2}$ and $\mathbf{6_{cyc}}\cdot\mathbf{H_2}$.

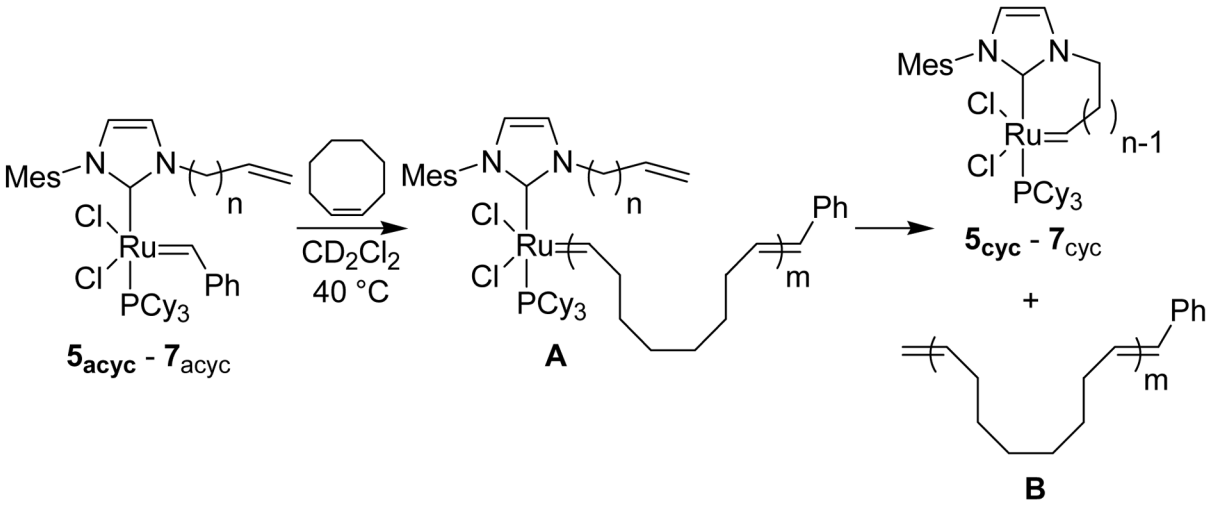

Scheme 4.
Proposed species observable upon ROMP of COE using open catalysts $\mathbf{5_{acyc}} - \mathbf{7_{acyc}}$.

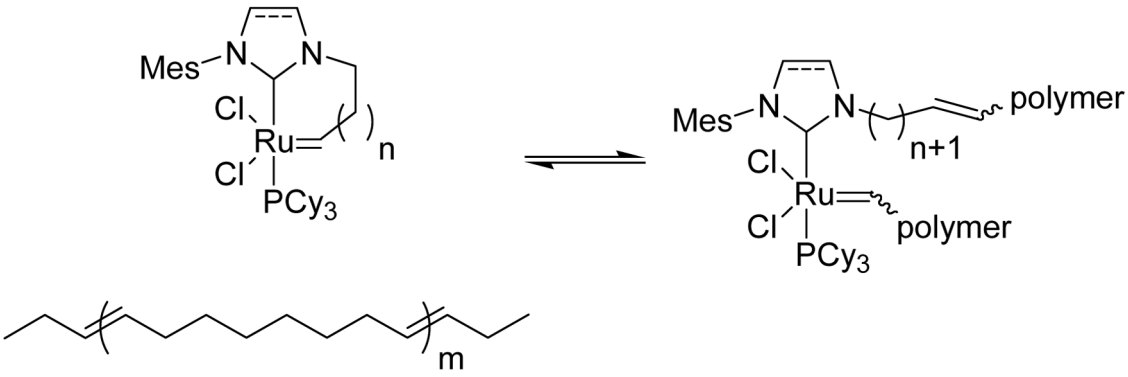

Scheme 5.
Equilibration of cyclic catalyst and linear PCOE.

Table 1

Cyclization to give cyclic catalysts **4_{cyc}** – **7_{cyc}**.[a]

cyclic catalyst	tether length	yield (%)[b]	
		0.01 M	0.001 M
4_{cyc}	4	62	81
5_{cyc}	5	76	97
6_{cyc}	6	81	97
7_{cyc}	7	0	63

[a] Reactions conducted in dry C_6D_6 under N_2 atmosphere at 80 °C for 1 h.

[b] Determined by ^1H NMR spectroscopy.

Table 2

Selected ^{1}H NMR and single-crystal X-ray data for $\mathbf{4_{cyc}}$ – $\mathbf{6_{cyc}}$, $\mathbf{5_{cyc}}\cdot\mathbf{H_2}$ and $\mathbf{6_{cyc}}\cdot\mathbf{H_2}$.

Catalyst	$\mathbf{4_{cyc}}$ [b]	$\mathbf{5_{cyc}}$ [b]	$\mathbf{6_{cyc}}$	$\mathbf{5_{cyc}}\cdot\mathbf{H_2}$	$\mathbf{6_{cyc}}\cdot\mathbf{H_2}$
		NMR data			
δ H2 (ppm)[a]	19.70	20.50	19.71	20.39	19.61
$^3J_{H2,P1}$ (Hz)[a]	14.1	10.5	5.1	9.3	5.0
		dihedral angles (°)			
Cl2-Ru1-C2-C3	51.3	26.6	16.2	18.3	21.1
N1-C1-Ru1-C2	156.5	162.2	153.5	160.0	151.2
		bond angles (°)			
C1-Ru1-P1	171.0	166.0	163.3	165.3	168.8
N1-C1-Ru1	128.8	127.0	126.6	124.3	124.0
N2-C1-Ru1	127.8	128.9	129.4	128.1	129.5
N1-C1-N2	103.4	104.1	103.6	107.5	107.2
		bond lengths (Å)			
Ru1-C1	2.076	2.091	2.113	2.072	2.084
Ru1-C2	1.812	1.806	1.823	1.821	1.800
Ru1-P1	2.402	2.421	2.421	2.417	2.423

[a] Data taken in C_6D_6 at ambient temperature.

[b] See ref 9.